This is a repository copy of *Engineering performance of a new siloxane-based corrosion inhibitor*.

White Rose Research Online URL for this paper:
http://eprints.whiterose.ac.uk/93481/

Version: Accepted Version

ENGINEERING PERFORMANCE OF A NEW SILOXANE-BASED CORROSION INHIBITOR

N. Holmes [1], R. O'Brien[2] and P. A. M. Basheer [3]

[1] Dublin Institute of Technology,

Department of Civil and Structural Engineering,

Bolton Street,

Dublin 1,

Ireland.

Phone +353(0)1 402 2914

Fax +353 (0)1 402 3720

Email niall.holmes@dit.ie

[2] Formerly with Queen's University Belfast,

School of Planning, Architecture and Civil Engineering,

Belfast,

Northern Ireland,

U.K.

[3] Queen's University Belfast,

School of Planning, Architecture and Civil Engineering,

Belfast,

Northern Ireland,

U.K.

ABSTRACT

This paper presents an evaluation of a new non-toxic corrosion inhibitor on selected engineering properties of concrete mixes with different cementitious materials following a corrosion and durability study on concrete samples. Corrosion inhibitors consist of powders or solutions which are added to concrete when mixed to prevent or delay corrosion of steel by their reaction with ferrous ions to form a stable and passive ferric oxide film on the steel surface. The new inhibitor functions slightly differently and its corrosion inhibition effect is due to the formation of a siloxane coating on the steel surface. Therefore, the performance of the new inhibitor in concrete mixes manufactured with CEM I, PFA and GGBS cements was compared against a well known and established corrosion inhibitor on the market, namely Calcium Nitrite in terms of their effect on workability (measured in terms of slump), compressive strength, freeze-thaw durability and macro-cell corrosion.

The results from this experimental programme have demonstrated that the new inhibitor is effective in reducing or slowing down corrosion. In addition, it was found that CEM I concrete containing the new inhibitor was less penetrable to chlorides than that without. A similar set of results was obtained for the freeze-thaw resistance, but the compressive strength was found to decrease with the addition of the new inhibitor. In the case of concretes containing PFA and GGBS, the new inhibitor was found to be less effective. Further, long-term investigations are recommended to assess the effectiveness over time.

KEYWORDS: corrosion inhibitor; corrosion; durability; calcium nitrite; encapsulated siloxane.

1. INTRODUCTION

Corrosion of embedded steel reinforcement is the most common and destructive form of deterioration found in concrete. To reduce or limit the effects of corrosion, inhibitors are occasionally used as an admixture at the time of manufacturing concrete. One of these products, and perhaps the most well known, is Calcium Nitrite (CN). This product, in liquid form in reinforced concrete, reacts with the ferrous ions to form a stable and passive ferric oxide film on the steel surface and thereby increases the critical threshold of chlorides required for corrosion to begin. Modern additives are required to be non-toxic and have no detrimental effects on the concrete fresh (workability and setting) and hardened (strength development) properties. Another important aspect to consider is their ease of use and how they are added to the concrete in batching plants. Corrosion protection agents or inhibitors that combine long term protection to the reinforcement against chloride attack with easy handling properties are rare. For this reason, a new type of corrosion inhibitor, based on siloxane, was developed by a German company.

The new inhibitor is easy to handle, non-toxic and consists of encapsulated siloxane in polyvinyl alcohol in powder form and can be added in dry form directly into the concrete mix without pre-mixing [1]. This results in a homogeneous and efficient dispersion of the encapsulated siloxanes. When water comes into contact with it in the concrete, the polyvinyl alcohol coating surrounding the powder is dissolved and the siloxane is evenly distributed throughout. Siloxane is a chemical compound consisting of elements of hydrogen (H), silicone (Si) and oxygen (O) and is represented in the form H_2SiO.

At high pH values (>12), such as those found in concrete, Si-oligomer of the siloxane hydrolyses and forms a protective layer at the surface of the reinforcement, as demonstrated in Figure 1. Similarly, at low pH values when steel is de-passivated, Si-oligomer also hydrolyses, which results in the re-passivation of the reinforcement, as illustrated in Figure 2.

The processes of corrosion due to chloride and carbonation mechanisms are well known. The most obvious method to reduce corrosion is to make the concrete less porous and less permeable, by improving the impenetrability (permeability, diffusion, absorption) of the cover-zone. Pore liners, such as siloxanes, act as an effective barrier to prevent the ingress of water and waterborne ions such as chlorides due their water repellent nature (hydrophobic characteristic). If the molecular size of the silaxanes is sufficiently big, they would block the capillary pores in concrete, thereby improve its impermeability [2].

They have been traditionally applied to exposed faces of concrete structures by brushing or spraying as their molecules are of similar size to water molecules, hence can penetrate into the capillaries of the cover concrete and adhere to the pore walls. They then react with adsorbed water along the pore walls to form a hydrophobic layer, which acts as a repellent to water and water-borne corrosive ions [2], but permit the flow of water vapour, allowing the treated concrete to dry out [3, 4]. They have been reported to have performed particularly well in improving the freeze-thaw resistance of the concretes here [4]. Therefore, it is to be expected that the admixed siloxanes from the new inhibitor should also perform as well to reduce the absorption of water and water-borne ions, whilst improving the freeze-thaw durability of concrete.

In order to assess the corrosion reduction properties of the new inhibitor, an experimental investigation was carried out at Queen's University Belfast, Northern Ireland. As the new inhibitor is siloxane-based and, as stated above, siloxanes are known to modify the pore system, it was decided to study the effect of the new inhibitor on compressive strength and durability performance of various concrete mixes in addition to its effect on macro-cell corrosion in concrete embedded with steel bars. The mixes included CEM I cement [5] and cementitious materials containing pulverised fuel ash (PFA) [6] and ground granulated blastfurnace slag (GGBS) [7] with and without the new inhibitor. Comparison mixes with Calcium Nitrite (CN) were also cast. The results of this study are reported and discussed in this paper.

3.   EXPERIMENTAL PROGRAMME

3.1 Mix Proportions

The concrete cast for this study included one control mix incorporating only CEM I cement and two other mixes containing CEM I + PFA and CEM I + GGBS both with a replacement level of 35%. A summary of the concrete cast is reported in Table 1. All of the mixes had a fixed w/c ratio of 0.55 and a cementitious material content of $400kg/m^3$. As the dosage of both PFA and GGBS was 35% of the total cementitious content, the differences in yield due to the differences in specific gravity of PFA and GGBS were taken into account by adjusting the quantity of the total aggregate content, whilst retaining the ratio of the coarse aggregate to the fine aggregate the same. Following a number of trial mixes, the final proportions were determined so that a slump between 100-150mm (S3 class slump) [8] could be achieved. The slump was adjusted by adding different dosages of a polycarboxylate based superplasticiser (SP). The mix proportions are summarised in Table 2.

3.2. Materials

CEM I cement complying with BS EN 197-1, 2000 [5], PFA conforming to BS 3892: Part 1 [6], and GGBS manufactured according to BS EN 15167-1 [7] were used as cementitious materials. Both the

fine and coarse aggregates were obtained from local sources in Northern Ireland. The fine aggregate used was medium graded sand [9] and the coarse aggregate was crushed basalt with a maximum size of 20 mm. Before mixing, the water absorption of the aggregates was determined and the water added to the concrete was adjusted accordingly to cater for this. For mixes containing SP, the water content in it was also calculated and the water added to the concrete was further corrected.

The recommended dosage of CN according to the suppliers was 20 l/m^3 (i.e. 24 kg/m^3) of concrete [10]. This is deemed to be suitable for anticipated chloride levels in a marine environment (approximately 1.2% by weight of cement). As recommended, a retarder [11] was also added to those mixes containing CN, at a dosage of 0.4% by weight of cement. The quantity of the new inhibitor was 4% by weight of cementitious materials.

3.3. Preparation of samples

The concrete was manufactured by following the procedure set-out in reference 8 using a pan mixer. For each mix in Table 1, 3 ponding slabs (250x250x100mm with a 10mm dyke), 3 regular slabs (250x250x100mm) for the freeze-thaw test cores and 9 cubes (100x100x100mm) were manufactured to determine the compressive strength at different ages for each mix. Each mix had a volume of 0.05m^3 including 10% for wastage.

Four 12mm diameter mild steel bars were cast into the ponding slabs (Figure 4(a)) so that half-cell potentials and macro-cell corrosion currents could be measured. The steel bars were prepared by cutting each to length (i.e. 290mm) and capped at each end with mortar (Figure 4(b)) to ensure corrosion was only occurring in that section of the bar encased in the concrete. Figure 4(c) demonstrates the final set-up for the ponding slabs before casting began.

After mixing, the concrete was poured, in 50mm thick layers, into the moulds and each layer was vibrated on a vibrating table for a time until no more air bubbles were visible on the surface. Curing of the concrete was provided by placing a polythene sheet over the specimens for 24 hours to trap moisture that evaporates from the surface. Following demoulding on day 1, the slabs were wrapped in damp hessian and placed inside polythene sheets for 7 days. They were then were transferred to a constant temperature room with ambient temperature and humidity of 20 ± 1^0C and $65 \pm 2\%$ respectively. After the cubes were demoulded, they were placed in water in a curing tank at $20 (\pm 1)^0C$ until they were tested.

After 7 days, the slabs were unwrapped and allowed the surface to dry in a constant temperature room $(20 (\pm 1)^0C)$ for 1 day so that a water-proof sealer could be applied to the four sides of the slabs, each receiving 3 coats, leaving the test surface and the surface opposite to it uncoated. After the paint had

dried, each ponding slab was placed in a water bath for 3 days to reduce the possibility of rapid absorption of the chlorides when ponding began.

3.4. Tests carried out

3.4.1. Workability
The workability (i.e. consistence) of the concrete was measured immediately after its manufacture in terms of slump. The test was carried out in accordance with BS EN 12350-2 [12].

3.4.2. Compressive strength
The compressive strength of the concrete was determined by crushing three 100mm cubes at 7, 28 and 56 days for each mix. The test was carried out according to BS EN 12390-3 [13].

3.4.3. Sorptivity
The water absorption (sorptivity) was measured using the Autoclam permeability system [14] (Figure 5). Tests were conducted on the 250x250x100mm concrete slabs at 49 days after they were dried in an oven for 14 days at a temperature of 40 ($\pm$ 1)^{0}C as recommended by Basheer et al. [15], at which point they were removed and allowed to cool at room temperature (20 ($\pm$ 1)^{0}C) for 24 hours before testing. It is known that the moisture content of concrete influences the transport of gases and liquids through porous materials [16, 17] and so all tests for measuring the transport properties should be carried out after preconditioning the test specimens. In the case of water absorption, the influence of moisture content is to reduce the transport and results from previous Autoclam sorptivity tests [16] have indicated that the effect can be reduced and reliable data obtained for laboratory studies if a preconditioning is employed, such as drying the concrete for 14 days in a 40^{0}C oven.

3.4.4 Corrosion Studies
The 250x250x100mm thick slabs, with the 10mm dyke (Figure 3), were subject to a weekly ponding regime using a 0.55M NaCl solution. This consisted of ponding the solution on the specimens for 24 hours and then removing for 6 days to allow drying in a constant temperature room with an ambient temperature and humidity of 20 ($\pm$ 1)^{0}C and 65 ($\pm$ 2)% respectively before being ponded again.

Once every week half-cell potentials in accordance with ASTM C876 – 09 [18] was carried out using a hand-held copper-sulphate solution apparatus (Figure 6). The positive lead was attached to the anodic (top) bar where a piece of the protecting mortar was removed (Figure 6) so that a connection could be made. As shown in this figure, a wetted sponge, attached to the tip of the electrode, was used to provide electrical conductivity between the electrode and the concrete surface. The potential across the cell was measured and recorded at one-third points from both ends of the bar along its length.

These values were compared with the guidance given in ASTM C876-09 (Table 3) to assess the probability of corrosion.

The corrosion of the anodic bar (top bar in Figure 3) was measured by using a macro-cell corrosion arrangement (Figure 7). When the anodic bar corrodes due to the action of chlorides penetrating from the ponded surface, a difference in potential occurs between it and the bottom steel, which acts as the cathode. The anodic steel which is corroding has a greater negative potential than the passive steel on the bottom, so a current flow occurs due to the connection between them by means of the 10Ω resistance. This current can be measured directly using a zero resistance ammeter or by measuring the potential across the 10Ω resistance and then calculating the corrosion current using Ohm's law (Equation 1).

$$i = \frac{V}{R}$$
<div align="right">Equation 1</div>

where i is the corrosion current in Amp, V is the potential measured across the resistance in Volt and R is equal to 10Ω. It may be noted that the potential measured across the resistance from the test slabs will be in millivolt and the corrosion current will be in milliamp.

3.4.5 Freeze-thaw Test

The freeze-thaw test was carried out using the RILEM TC-117 procedure [19] on 70mm long x 100mm diameter cylindrical specimens cored from the slabs. The cores were prepared by painting the curved surface with three coats of a water proof coating as specified in the procedure. The top and bottom surfaces were not coated with the paint. At this stage, they were placed in specially designed containers for 7 days with the test face down and the core dipped up to a depth of 15mm in a 3% sodium chloride solution. Before inserting the specimens into the freeze-thaw chamber the level of the solution was reduced from 15mm to 5mm. The freeze thaw chamber was programmed with a 12 hour cycle, as shown in Figure 8. After 14 cycles (or 7 days) the cores were removed and the test surfaces were brushed into the container removing any loose material and weighed. The sample was replaced back into the chamber and repeated for a further 14 cycles, after which the cores were removed again and the weight of the brushed off material measured. An average of three cores were tested for each mix in Table 1.

4. RESULTS AND DISCUSSION

4.1. Workability

The slump values are reported in Figure 9. It can be seen that the majority of the measured slump was within the target range of 100–150 mm with a slight increase with the addition of the new inhibitor (mixes 1B, 2B and 3B). However, for those mixes with CN (1C, 2C and 3C), the measured slumps were far in excess of what was required. This was unexpected because it has been reported [20] that the addition of CN does not increase slump values even in higher w/c ratio concretes. Therefore, it is probable that the addition of the retarder in this investigation was not effective to control the slump retention. This is an area where further investigation is required.

4.1. Compressive strength

The compressive strength results are presented in Figures 10 to 12. As shown, when the new inhibitor (NI) was added to the mixes, there was a reduction in strength, except at 7 days for the CEM I only mix. This reduction is most evident at all ages when the new inhibitor was added to the PFA (2B) and GGBS (3B) mixes, as may be seen in Figures 11 and 12 respectively.

This reduction is possibly due to two reasons. Firstly, the Poly Vinyl Alcohol (PVA) and oligomeric polysiloxane (OP) within the new inhibitor assists in dispersing the powder in the concrete mix, allowing it to be available at sites where cement hydration takes place. Secondly, PVA may also retard the hydration process of the cement as a hydrophobic layer can form around the cement particles and create a barrier to water, leading to reduced strength development and lower compressive strengths over time. However, if water reacts with the cement particles before the condensation reaction of siloxanes takes place, cement particles could hydrate as normal and strength can develop, albeit slightly retarded.

Furthermore, the 4% of the new inhibitor used here may be too high for the corrosion protection required from an inhibitor. In most cases, a lower quantity of 2 to 3 % would be sufficient, which might reduce the detrimental effect on strength development. Previous work in this area with a 2% content of the new inhibitor [21] has shown to have little effect on compressive strength. In this context, further research is required to determine the most efficient quantity of the new inhibitor for different concretes used in different exposure environments.

For the mixes containing CN, there was a slight increase in the strength of the concrete at all ages, despite it giving a higher slump value for the three types of concretes. This increase can be attributed to its water reducing effect. Previous research [21] has also shown an increase in compressive strength

by adding CN, with an average 12–13% increase than similar mixes without it. The increase in compressive strength for CEM I and GGBS mixes at 28 days due to the addition of CN was 6-12%.

4.2. Sorptivity

The sorptivity values of the mixes are reported in Figure 13. In all cases, it is clear that concrete with the new inhibitor (1B, 2B and 3B) have significantly lower sorptivity values than all other mixes. Unexpectedly, the results indicate that the CEM I concretes have better sorptivity properties than both the PFA and GGBS concretes containing the new inhibitor and CN. These tests were carried out at 49 days of age following 14 days of drying in an oven at 40^0C, as recommended by Basheer et al [15]. It is expected, and has been shown previously [22] that the sorptivity values will reduce with age in mixes with supplementary cementitious materials due to the ongoing hydration and pozzolanic reactions over time.

In terms of corrosion resistance in a marine environment, a low sorptivity can reduce the amount of chlorides that can be absorbed by the near surface concrete and, hence, that which can be transported through the concrete via diffusion (under a concentration gradient). The new inhibitor was originally proposed to improve the corrosion resistance property of concrete by surrounding the reinforcement with a protective layer. However, it is clear that, whilst it is effective in improving the sorptivity.

4.3 Corrosion Monitoring

The average results from the weekly half-cell and macro-cell monitoring programme during ponding are shown in Tables 4 and 5. Half-cell potential measurement as a method to assess the likelihood of corrosion occurring has gained confidence following the creation of the ASTM standard C876 [18]. This standard provides guidelines (Table 3) to evaluate if corrosion is occurring. As may be seen, potentials less than -350mV have a high probability (>90%) of corrosion occurring.

The half-cell potentials are considered along with the macro-cell corrosion current values to provide a comprehensive assessment if corrosion is occurring. Figures 14-16 present the half-cell potentials and macro-cell corrosion current values for CEM I cement mixes 1A-C respectively. Figures 17-19 show the corresponding values for PFA mixes 2A-C and Figures 20-22 show the corresponding values for the GGBS mixes (3A-C).

As may be seen in Figures 14-16, and somewhat expected, CEM I Mix 1A has higher negative half-cell potentials and notable macro-cell corrosion current values compared to CEM I mixes 1B and 1C. However, mix 1B has the lowest negative half-cell potentials and macro-cell corrosion current results, with the half-cell readings remaining between -50 and -100mV throughout the weekly ponding regime. The CEM I Mix 1C has higher negative half cell readings than mix 1B containing the new

inhibitor and appears to be increasing marginally over time, but less so than mix 1A. A similar trend was found for mixes containing PFA and GGBS as shown in Figures 17-19 and 20-22 respectively.

The mixes with no corrosion inhibitor, 1A, 2A and 3A in Figures 14, 17 and 20 respectively, all had a high negative half cell potential and they all indicated active corrosion, as per Table 4. This was further confirmed with the presence of measurable corrosion current for these mixes. However, for both sets of mixes containing corrosion inhibitor (1B, 2B and 3B and 1C, 2C and 3C), there was no measurable corrosion current. In the case of mixes containing the new inhibitor, the half cell potential values remained almost constant at a value between -50 and -150mV throughout the test duration. It is highly unlikely that the steel bars embedded in these mixes are corroding, which is confirmed by the zero corrosion current values in Table 5.

The increase in more negative half-cell potentials of mixes containing CN (Figures 16, 19 and 22) may suggest high probability of corrosion (Table 4). However, this is not the case, as indicated by the zero corrosion current values. CN is known to increase the critical threshold of chlorides required before corrosion can begin and, therefore, half-cell potentials alone cannot be used as an indication of corrosion activity for mixes containing CN. For this reason, it is not unexpected that these trends are seen as compared to Figures 14, 17 and 20 that show an increase in half-cell potentials with a corresponding increase in macro-cell current.

A review of the values in Table 4 would suggest that the half-cell potentials became more negative with increase in duration of ponding for all of the control mixes (that is, mixes containing no inhibitors) irrespective of the binder type. When the half cell potentials of PC, PFA and GGBS are compared for the control containing no corrosion inhibitor, the benefit of the supplementary cementitious materials is not obvious. The corrosion current values in Table 5 also followed a similar trend. This may be due to the fact that for the benefit of supplementary cementitious materials for reducing the rate of corrosion to become clearer, longer-term experimentation is required.

4.4 Freeze-thaw resistance
The accelerated freeze thaw test was carried out on 3 cores per concrete mix for the CEM I and PFA mixes with the ultrasonic pulse transit time of each core measured before and after the test. The transit time for the cores from mixes 1A-C and 2A-C before and after the test and an average increase in transit time as shown in Table 6 for ease of interpretation. Increased transit times after testing would indicate the formation of micro-cracking from hydrostatic pressure caused by the expansion of water within the capillary pores from the freeze-thaw cycles. The weight of the dried residuals from the cores are shown in Table 6. The cores from mixes 2A and 2C were severely deteriorated to the point

where almost a third of them had totally disintegrated (Figure 23). As a result, the ultrasonic pulse velocity (UPV) readings were not measurable in mix 2A and are denoted "Unreadable" in Table 6.

In Table 6, an increase in transit time was observed for all cores and is considered to be due to micro-cracking caused by the internal expansive pressures exerted on the microstructure of the concrete during the freeze-thaw cycles. The extremely high variations in transit time for mixes 2A and 2C are considered to be the result of micro-cracking near the exposed surface of the cores.

To assess the performance of the various mixes during the freeze-thaw cycles, the residual material was brushed off each core and weighted after the test and are summarised in Table 6 and shown in Figure 24. Figure 25 shows the average transit time for the six mixes, which indicate the formation of micro-cracks. It is clear that those concrete mixes containing the new inhibitor (mixes 1B and 2B) have performed better than all others in the study. This is considered to be due to their low absorption characteristics, as demonstrated by the sorptivity values in Figure 14.

5.   CONCLUSIONS

On the basis of the various investigations carried out to assess a new siloxane based corrosion inhibitor, the following conclusions have been drawn:

(1)   The new corrosion inhibitor has been found to be effective in preventing corrosion of steel in concrete containing CEM I, PFA and GGBS. Over the duration of this study using accelerated corrosion regimes (due to chloride ponding), no evidence of corrosion was found using the half-cell potential and macro-cell corrosion current measurements.

(2)   The sorptivity tests have indicated that the concretes containing the new inhibitor were less penetrable to water than other concretes in the study. This suggests that it alters the pore structure in such a way that the pores become non-sorptive. Correspondingly, the freeze-thaw durability was found to be improved with the use of the new inhibitor in concretes containing CEMI, PFA and GGBS.

(3)   It has been demonstrated that the inclusion of the new inhibitor in this study yields a decrease in its compressive strength of approximately 12 MPa in all concrete mixes at 7, 28 and 56 days. This may be due to the formation of oligomeric polysiloxane which forms a hydrophobic layer around the cement particles, inhibiting their hydration when the dosage of the inhibitor was 4% by weight of the cementitous materials. Further investigations to identify the most suitable dosage for different cementitious materials and concretes for different exposure environments are required.

6.   ACKNOWLEDGEMENTS

7.   REFERENCES

[1]   Schottler, M., ELOTEX® COPRA900, A corrosion protection agent in powder form, 29th Cement and Concrete Science Conference, Leeds, 2009.

[2]   Basheer, P.A.M. and Long, A.E., "Protective qualities of surface treatments for concrete", Structures and Buildings, The Institution of Civil Engineers, 1997, August, 122 (3), pp 339-346. ISSN 0965-0911.

[3]   Basheer, L, Cleland, D.J. and Long, A.E, Protection provided by surface treatments against chloride induced corrosion, Materials and Structures, 1998, 31: 459-464.

[4]   Basheer, L and Cleland, DJ., Freeze-thaw resistance of concretes treated with pore liners, Construction and Building Materials, 2006, 20: 990-998.

[5]   BS EN 197-1, Cement: Composition, Specifications and Conformity Criteria for Common Cements, British Standards Institution, London, 2000.

[6]   BS 3892-1, Pulverized-fuel ash. Specification for pulverized-fuel ash for use with Portland cement, 1997.

[7]   BS EN 15167-1, Ground granulated blast furnace slag for use in concrete, mortar and grout. Definitions, specifications and conformity criteria, 2006.

[8]   BS EN 206 Part 1, Concrete: Specification, performance, production and conformity, British Standard Institute, 2000.

[9]   BS EN 12620, Aggregates for concrete British-Adopted European Standard, 2007.

[10] Larsen Building Products, Technical Data Sheet for Calcium Nitrite admixture, CR 800, 2008.

[11] Larsen Building Products, Technical Data Sheet for Retarder, Chemcrete for CR 800, 2008.

[12] BS EN 12350-2, Testing fresh concrete. Slump-test, 2009.

[13] BS EN 12390-3, Testing hardened concrete. Compressive strength of test specimens, 2009.

[14] Basheer PAM., Long AE and Montgomery FR, 'The Autoclam – a New Test for Permeability. Concrete', Journal of the Concrete Society, 1994: 27–29.

[15] Basheer, PAM, Nolan, EA, McCarter, WJ and Long, AE, Effectiveness of in-situ moisture pre-conditioning methods for concrete, Journal of Materials in Civil Engineering, 2000: 131-138.

[16] Basheer, PAM, Nolan, E, Near-surface moisture gradients and in situ permeation tests, Construction and Building Materials, 2001, 15: 105-114.

[17]   Technical Report No. TR-31, Permeability testing of site concrete, The Concrete Society, 2008, 90 pp.

[18]   ASTM C876, Standard test method for half-cell potentials of uncoated reinforcing steel in concrete, Annual Book of ASTM Standards, 1999, 14.

[19]   TC 117-FDC Recommendation, Test method for the freeze thaw and deicing resistance of concrete, Materials and Structures, 1996, 29(193): 523-528.

[20]   Soylev, TA and Richardson, MG., Corrosion inhibitors for steel in concrete: State of the art report, Construction and Building Materials, 2008, 22: 609-622.

[21]   Frankfurt University of Applied Sciences Test Report 'Preliminary investigations for the use of the concrete additive ELOTEX COPRA 900 within the scope of a pilot project, 2008.

[22]   Elahi, A, Basheer, PAM, Nanukuttan, SV and Khan, QUZ, mechanical and durability properties of high performance concretes containing supplementary cementitious materials, Construction and Building Materials, Vol. 24, 292-299, 2010

Table 1   Summary of concrete cast

Mix ID	Description
1A	CEM I cement
1B	CEM I cement with new inhibitor
1C	CEM I cement with CN
2A	CEM I cement + 35% PFA
2B	CEM I cement + 35% PFA with new inhibitor
2C	CEM I cement + 35% PFA with CN
3A	CEM I cement + 35% GGBS
3B	CEM I cement + 35% GGBS with new inhibitor
3C	CEM I cement + 35% GGBS with CN

Table 2   Mix proportions

Mix ID	a/b	FA/CA	Mass of Ingredients (kg/m^3)								
			Water	CEM I	FA	CA		PFA	GGBS	CN*	New inhibitor
						10mm	20mm				
1A	4.24	0.54	245.86	400	595.37	385.85	714.39				
1B	4.12	0.55	245.28	400	581.88	377.10	698.20				16
1C	4.23	0.54	231.56	400	594.02	384.97	712.77			24	
2A	4.22	0.54	245.73	260	592.21	383.80	710.60	140			
2B	4.12	0.54	245.14	260	578.72	375.06	694.41	140			16
2C	4.21	0.54	231.43	260	590.87	382.93	708.99	140		24	
3A	4.23	0.54	245.73	260	592.21	388.80	710.60		140		
3B	4.12	0.54	245.14	260	578.72	375.06	694.41		140		16
3C	4.21	0.54	231.43	260	590.87	382.93	708.99		140	24	

FA – Fine aggregate, CA – Course Aggregate, PFA – Pulvarised fuel ash, GGBS – Ground granulated blast-furnace slag, a/b – aggregate-binder ratio

* In all cases where CN was used (mixes 1C, 2C and 3C), a retarder was added to the concrete at a dosage of 1.60kg/m^3. As the retarder contained 40%, this was also taken into account whilst determining the total water content for each mix.

Table 3   ASTM C876 Guidelines on half-cell potential readings [18]

Half-cell potential reading	Corrosion activity
Less negative than -200mV	>90% probability of no corrosion
Between -200 and -350mV	An increasing probability of corrosion
More negative than -350mV	>90% probability of corrosion

Table 4   Half-cell potential values for various mixes

Mix ID	Week	1	2	3	4	5	6	7	8	9
PC	1A	-86	-276	-250	-266	-275	-269	-303	-323	-430
	1B	-82	-64	-63	-63	-66	-65	-76	-89	-103
	1C	-95	-210	-192	-183	-200	-205	-209	-233	-262
PFA	2A	-99	-256	-276	-322	-310	-360	-401	-422	-420
	2B	-207	-173	-150	-129	-128	-83	-74	-74	-69
	2C	-110	-172	-196	-173	-190	-216	-274	-301	-333
GGBS	3A	-94	-275	-307	-329	-354	-389	-423	-456	-497
	3B	-133	-136	-116	-99	-104	-66	-86	-102	-145
	3C	-113	-181	-179	-193	-202	-254	-309	-336	-376

Table 5   Macro-cell corrosion current (milli-amps) for various mixes

Mix ID	Week	1	2	3	4	5	6	7	8	9
PC	1A	0.010	0.0167	0.020	0.0233	0.0267	0.0300	0.0367	0.0367	0.040
	1B	0	0	0	0	0	0	0	0	0
	1C	0	0	0	0	0	0	0	0	0
PFA	2A	0.010	0.0167	0.0167	0.020	0.0233	0.030	0.0333	0.0367	0.0433
	2B	0	0	0	0	0	0	0	0	0
	2C	0	0	0	0	0	0	0	0	0
GGBS	3A	0.010	0.0167	0.0367	0.0433	0.050	0.061	0.071	-0.085	-0.101
	3B	0	0	0	0	0	0	0	0	0
	3C	0	0	0	0	0	0	0	0	0

Table 6   Freeze-thaw results

Mix ID	Average weight of concrete removed (g)	Average transit time before test (µsec)	Average transit time after test (µsec)	Average increase of transit time (µsec)
1A	49.9	17.97	34.47	16.5
1B	2.23	17.87	22.63	4.76
1C	51.63	16.97	27.87	10.9
2A	203.27	17.23	Unreadable	-
2B	1.5	20.67	24.27	3.6
2C	63.9	18.47	41.9	23.43
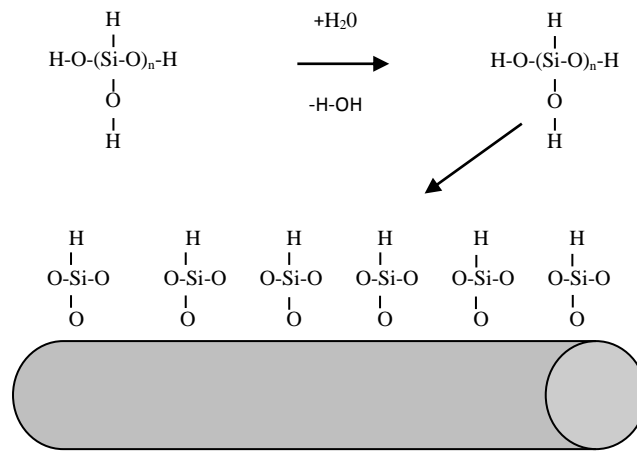
Figure 1   Illustration of hydrolysis of Si-oligomer [1]
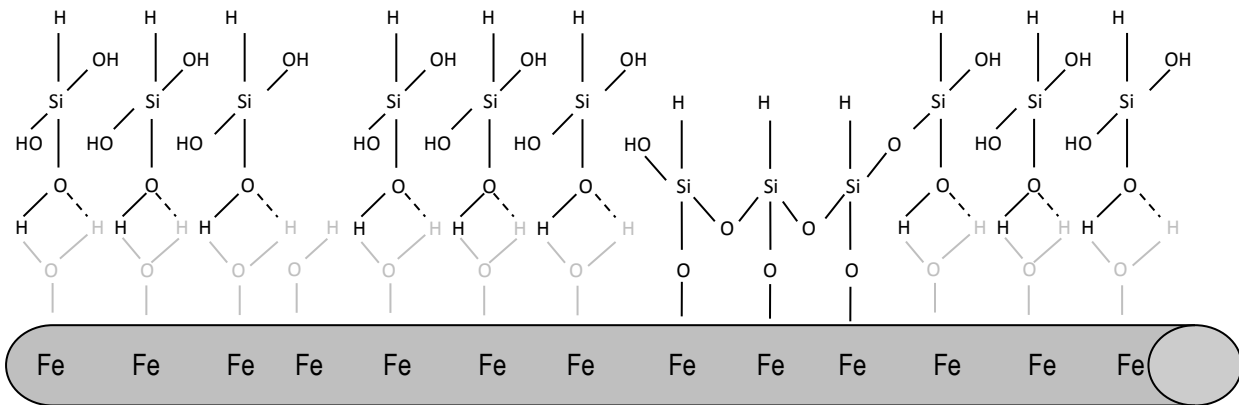
Figure 2   Illustration of re-passivation characteristic of the new inhibitor [1]
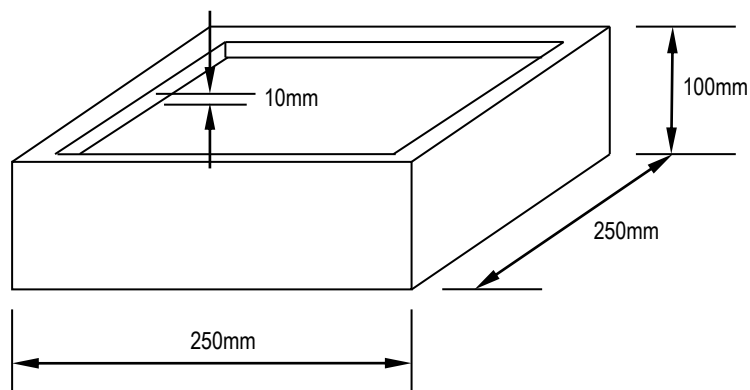
Figure 3   Concrete specimens with the 10mm dyke

(a)

(b)   (c)
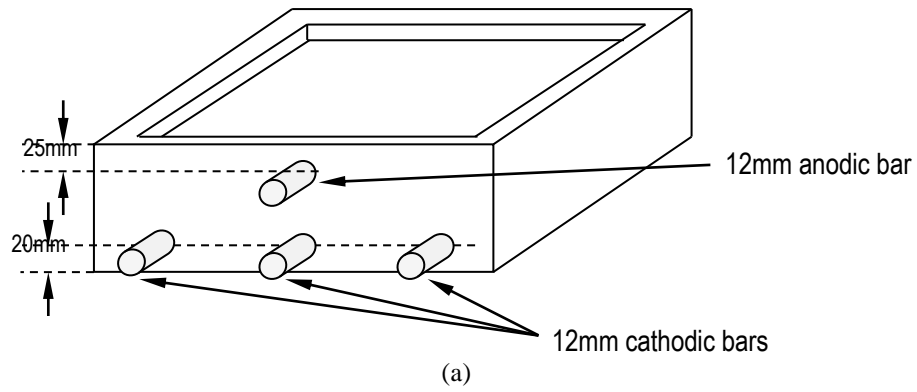
Figure 4   (a) Concrete ponding specimens, (b) anodic and cathodic bars and (c) bars placed in
the mould for embedding in concrete to measure half-cell potentials and macro-cell
current (also shown are electrodes for measuring the electrical resistivity of concrete)

Figure 5   Autoclam permeability apparatus [14]

Figure 6　　　　　　　　Half-cell potential test
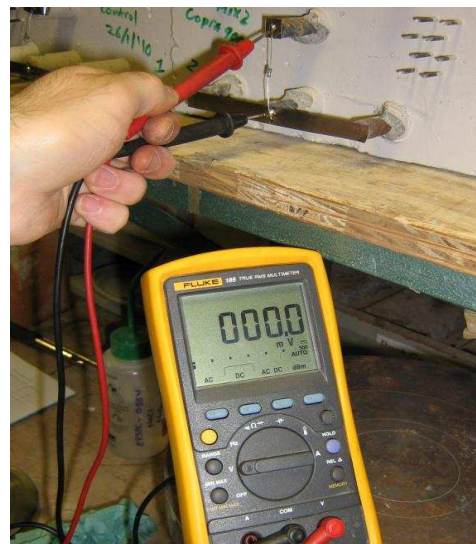
| (a) | (b) |

Figure 7　　Macro-cell corrosion measurement; (a) test specimen connected with 10Ω resistance connecting the anodic and cathodic bars and (b) measuring the voltage drop across the 10Ω resistance to calculate the corrosion current
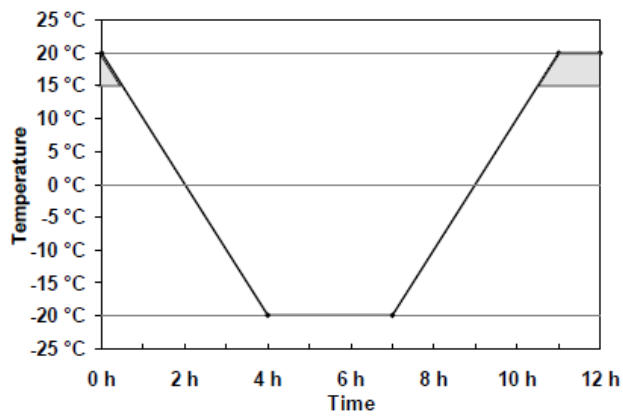
Figure 8   Freeze thaw cycle for RILEM test [19]
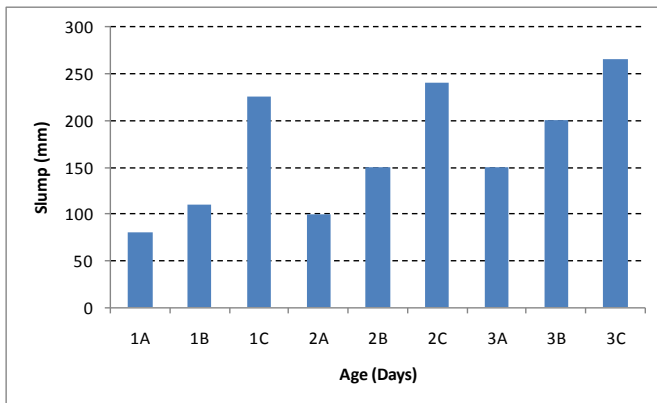
Figure 9   Slump values
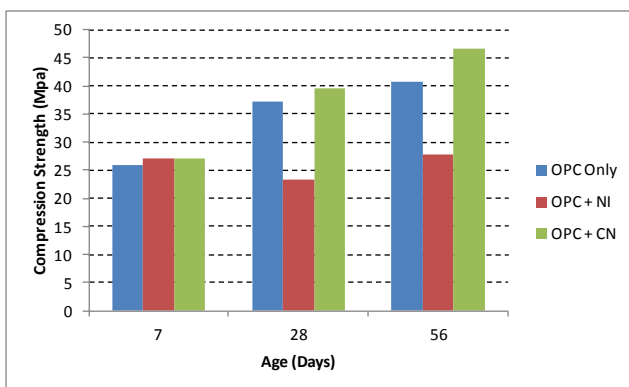
Figure 10   Compressive strength results for the PC concretes with the new inhibitor and CA

20
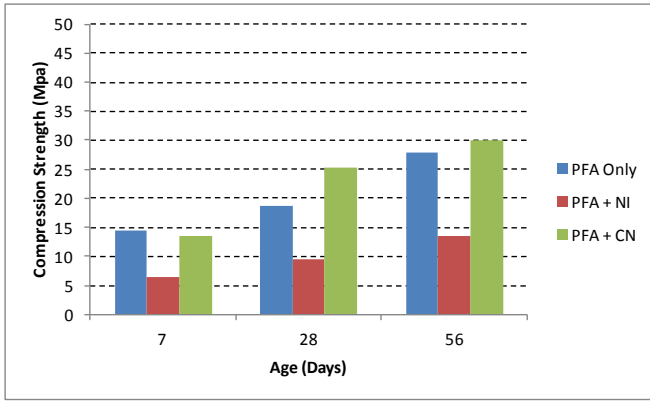
Figure 11　　　　Compressive strength results for the PFA concretes with the new inhibitor and CA
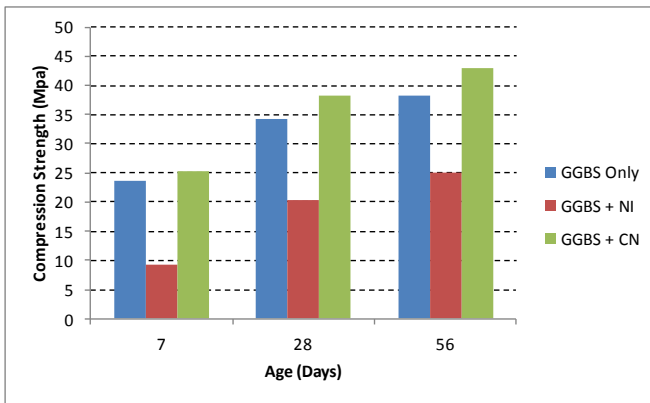
Figure 12　　　　Compressive strength results for the GGBS concretes with the new inhibitor and CA
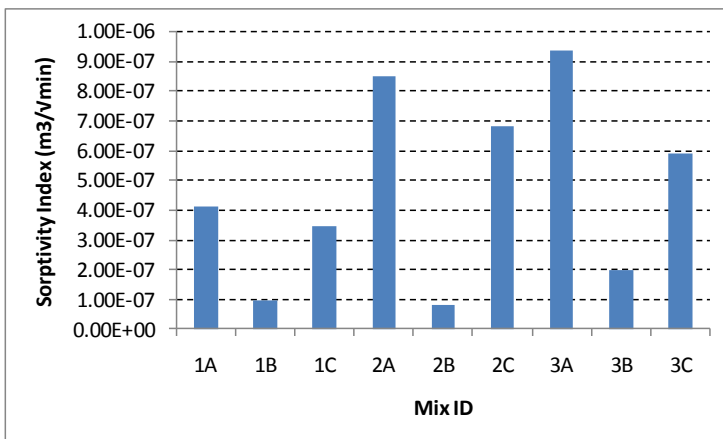
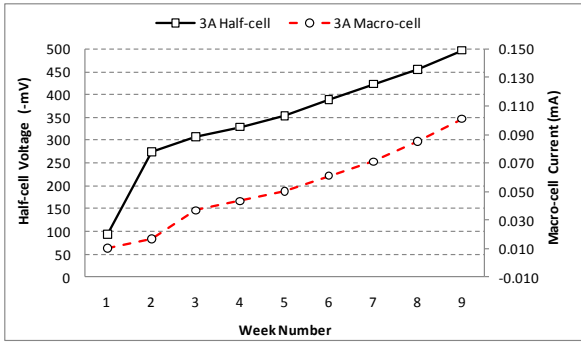**Figure 13**　　　　Sorptivity indices of the various mixes

21
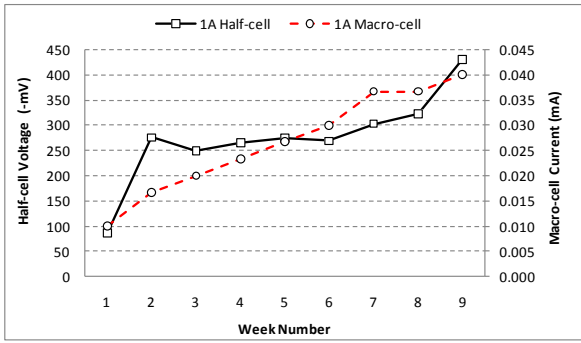
Figure 14 Half-cell potential and macro-
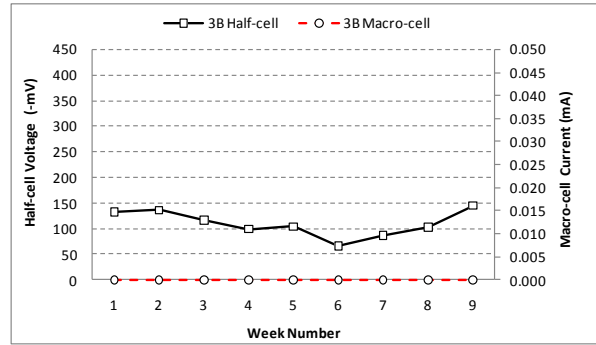cell corrosion current values for mix 1A (PC)
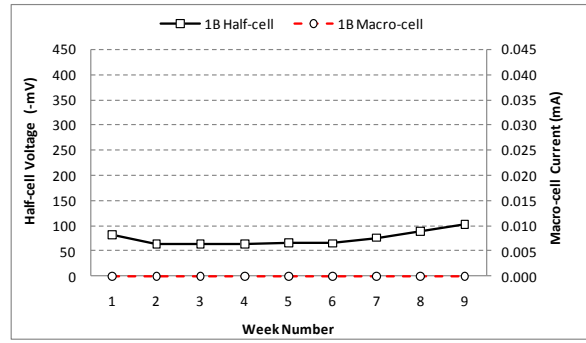
Figure 15 Half-cell potential and macro-
cell corrosion current values for mix 1B
(PC+new Inhibitor)
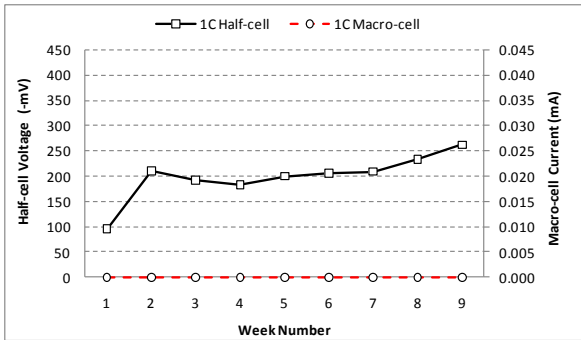
Figure 16 Half-cell potential and macro-
cell corrosion current values for mix 1C
(PC+CN)
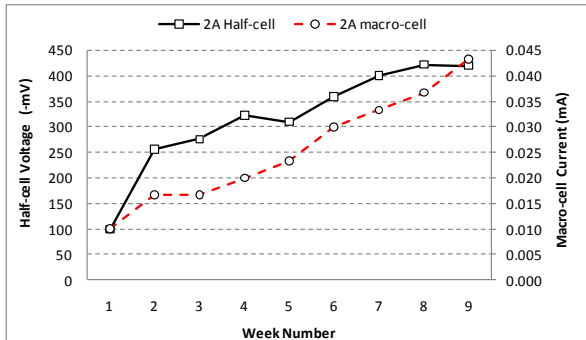
Figure 17 Half-cell potential and macro-cell
corrosion current values for mix 2A (PFA)
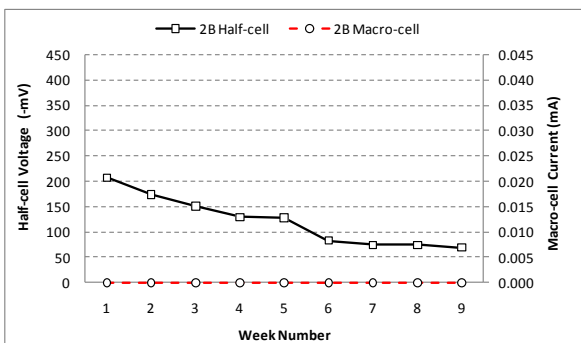
Figure 18 Half-cell potential and macro-
cell corrosion current values for mix 2B
(PFA+new inhibitor)
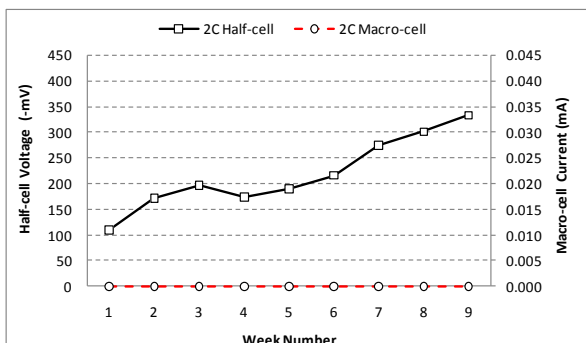
Figure 19 Half-cell potential and macro-cell
corrosion current values for mix 2C (PFA+CN)

Figure 20 Half-cell potential and macro-
cell corrosion current values for mix 3A (GGBS)

Figure 21 Half-cell potential and macro-cell
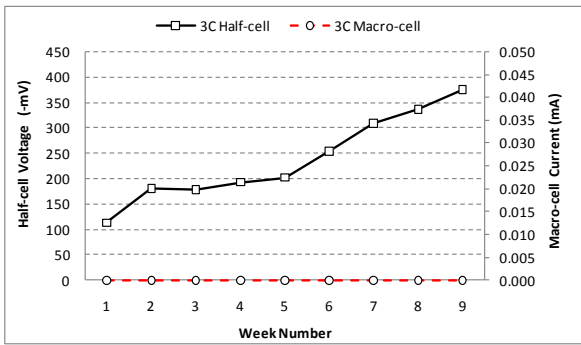corrosion current values for mix 3B (GGBS+new
inhibitor)

Figure 22 Half-cell potential and macro-cell
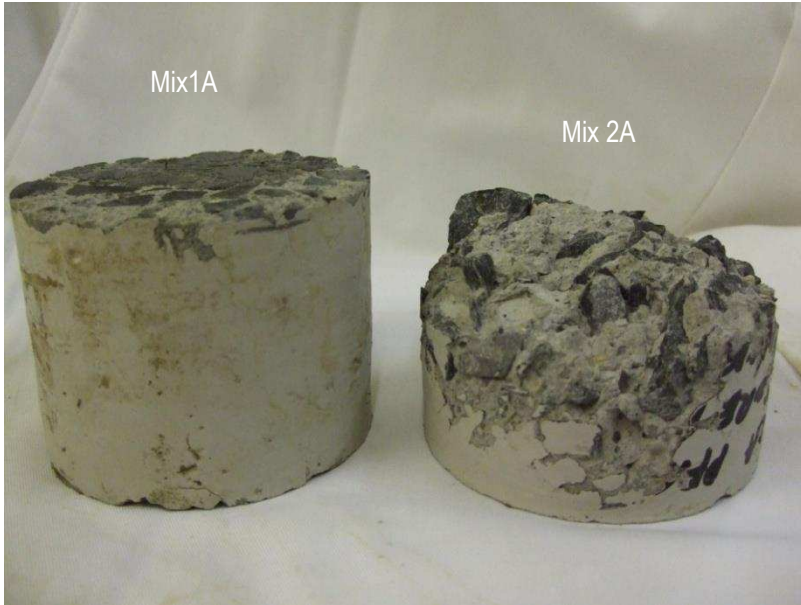corrosion current values for mix 3C (GGBS+CN)

Figure 23   Comparison between a relatively undamaged core and a severely damaged following the freeze-thaw test

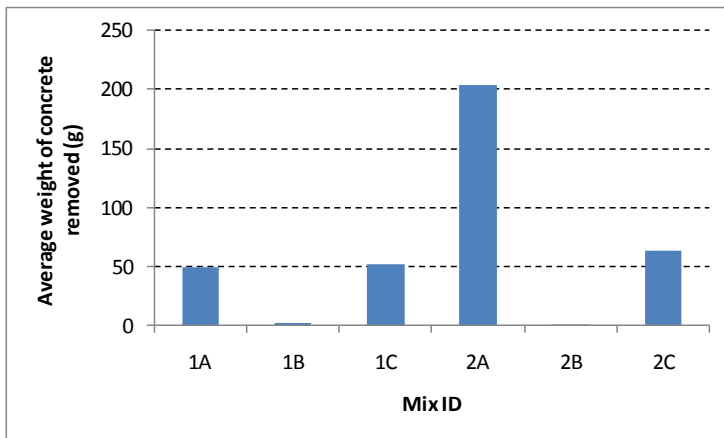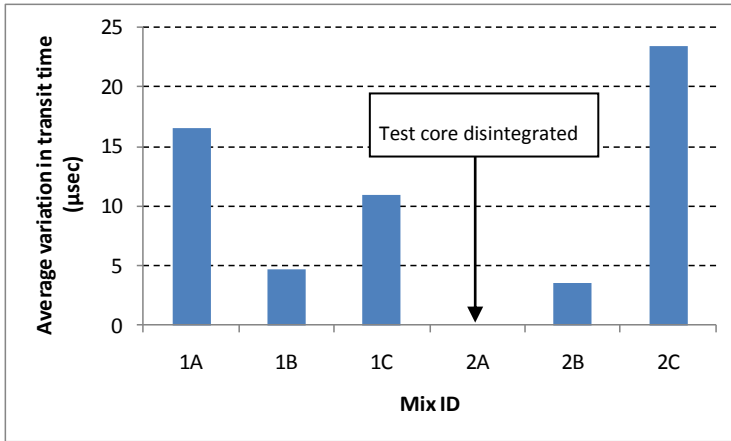**Figure 24**   Average weight (g) of concrete removed after freeze-thaw testing

Figure 25   Average variations in transit time